journal

J. Am. Ceram. Soc., 78 [6] 1640–48 (1995)

In Situ Fluorescence Probing of the Chemical Changes during Sol–Gel Thin Film Formation

Fumito Nishida,*,† John M. McKiernan,‡ Bruce Dunn,*,† and Jeffrey I. Zink‡

Department of Materials Science and Engineering and Department of Chemistry and Biochemistry, University of California, Los Angeles, California 90024

C. Jeffrey Brinker*,§,¶ and Alan J. Hurd§

Sandia National Laboratories, Albuquerque, New Mexico

Department of Chemistry and Department of Chemical Engineering, University of New Mexico, Albuquerque, New Mexico

Pyranine (8-hydroxy-1,3,6-trisulfonated pyrene) was used as an *in situ* fluorescence probe to monitor the chemical evolution during sol–gel thin film deposition of silica by the dip-coating process. The sensitivity of pyranine luminescence to protonation/deprotonation effects was used to quantify changes in the water/alcohol ratio in real time as the substrate was withdrawn from the sol reservoir. The spatially resolved spectral results showed that preferential evaporation of alcohol occurred, and that the solvent composition in the vicinity of the drying line reached values in excess of 80 vol% water. Correlation of the luminescence results with the interference pattern of the depositing film allowed the solvent composition to be mapped as a function of film thickness.

I. Introduction

THE sol–gel process is a method of preparing inorganic oxide glasses and ceramics from polymeric or colloidal sols at temperatures well below those used in traditional processing techniques.[1–3] Interest in sol–gel thin films has grown in recent years as a number of applications have emerged in areas such as protective and optical coatings, high and low dielectric constant films, electrochromics, waveguides, ferroelectric thin films, sensors, and membranes.[4] The films can be produced readily by several different methods including spin coating and dip coating.[5] Dip coating is perhaps more important technologically since a uniform coating can be deposited onto substrates of large dimensions and complex geometries. In the dip-coating process the substrate is immersed into the coating sol and then withdrawn at a constant rate. Brinker, Hurd, and co-workers have carried out extensive work, both experimental and theoretical, and have established how various physical and chemical parameters involved in dip coating affect the structure and properties of the final film.[5]

In the dip-coating process, a substrate is withdrawn slowly at constant speed (typically 10–20 cm/min) from a sol which contains polymeric or colloidal species in suspension (see Fig. 1). A liquid film becomes entrained on the surface of the moving substrate. This film thins by solvent evaporation accompanied by gravitational draining and, for multicomponent fluids, possible surface tension gradient driven flows. When the upward moving flux is balanced by that of evaporation, a steady, film profile, 1–2 cm in height, is established which terminates at a drying line. Although the entrained film profile is long (1–2 cm) and thin (0.1–4 μm), giving it a wedge shape, a magnified view of a typical ethanol/water/silica film (Fig. 1) shows two parabolic shapes corresponding to the preferential evaporation of ethanol to create a water-rich film, which subsequently dries to produce the deposited film. The steady-state film profile shows (Fig. 1) the complete sol to gel to xerogel transformation. Spatially resolved chemical, structural, and rheological characterization of this situation therefore should allow us to understand the genesis of sol–gel-derived films as well as gain insights into sol–gel processing.

The structural evolution in sol–gel thin films is very complex. Unlike the bulk gel system where gelation, aging, and drying occur sequentially over a period of several weeks or longer, all of these processes typically occur within 30 s in the thin film. The result is that the drying stage of the sol–gel process overlaps the aggregation/gelation and aging stages. The final structure of the sol–gel thin film is affected by several chemical and physical parameters. However, the most critical issue affecting the final film structure is the competition between phenomena which collapse the film, such as evaporation and capillary pressure, and phenomena which tend to stiffen the structure, such as condensation and aggregation.

Determining the composition of the film at different stages during film formation is central to understanding how the changing chemical and physical conditions affect the film's properties and microstructure. The composition of the sol (e.g., ethanol, water, and silica precursor) is quite different from that of the final film (silica), and, although models have been developed to consider this evolution, only limited experimental work has addressed this topic. Monitoring the film evolution requires *in situ* observation of composition changes. These changes in chemistry, in turn, affect the surface tension, capillary pressure, and condensation rate, and therefore the densification of the network. To date, the characterization of sol–gel thin films has generally been limited to the characterization of the final dried film. Such methods, however, offer only indirect information regarding the physical and chemical evolution during thin film formation. One example of an *in situ* monitoring technique was the imaging ellipsometry measurements of Hurd and Brinker which measured film thickness and refractive index during film deposition.[6]

This paper reports new results on the use of a luminescent molecule to monitor the chemical evolution *in situ* during thin

L. C. Klein—contributing editor

Manuscript No. 193564. Received May 20, 1994; approved December 27, 1994.
Supported by the National Science Foundation (DMR 9003080) and by the Department of Energy Basic Energy Sciences Program. Sandia National Laboratories is a Department of Energy facility operated under Contract No. DE-AC04-76-DP00789.
*Member, American Ceramic Society.
†Department of Materials Science and Engineering, University of California.
‡Department of Chemistry and Biochemistry, University of California.
§Sandia National Laboratories.
¶University of New Mexico.

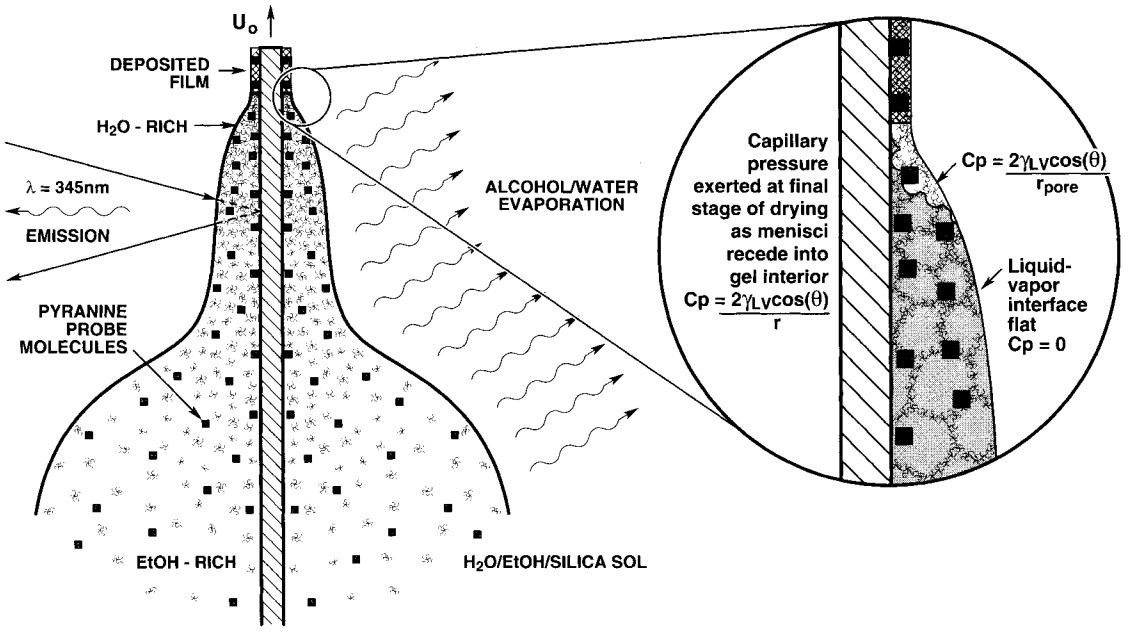

Fig. 1. Schematic of sol–gel dip coating. Withdrawal of the substrate at speed U_0 from an alcohol–water–silica precursor sol entrains a film that thins by evaporation and draining. The shape of the film profile is steady in time and reflects the preferential evaporation of alcohol to leave a water-rich sol. Further evaporation causes collapse of the inorganic deposit due to capillary forces leading to the final deposited film. Spatially resolved fluorescence spectroscopy of entrained pyranine molecules provides information concerning the local chemical environment of the probe molecules as they are transported from the dilute sol to the depositing film.

film deposition by the dip-coating method. The incorporation of organic, organometallic, and biological molecules as dopants in sol–gel matrices has been well established in recent years.[7–9] This synthesis approach has led to a number of new optical materials. However, another important direction for this work has been to use luminescent molecules as optical probes of the sol–gel process. In the latter case, spectroscopic studies on bulk sols and gels have provided substantial insight regarding certain aspects of sol–gel chemistry (polarity,[10] pH,[11,12] water content[13,14]) and structural development.[15] Although there is a question of whether optical probe techniques can be adapted generally to thin films because of the shorter path length, the present work establishes that at least one fluorescent molecule may be applied very effectively to the characterization of thin films.

The fluorescent probe molecule, pyranine (8-hydroxy-1,3,6-trisulfonated pyrene), is sensitive to proton transfer phenomena. The fluorescence spectrum of this molecule is dependent upon protonation, with the protonated form having an emission maximum at 430 nm and the deprotonated form having a maximum at 515 nm.[16,18] The fundamental photochemistry of the molecule is well known, and it has found wide use as a pH indicator.[16–18] In previous studies with sol–gel materials, pyranine was used successfully to measure the alcohol/water content of aluminosilicate gels during the sol–gel—xerogel transformation and to study the effect of pH on water consumption during the gelation of a silica system.[13,14]

The present work extends the use of pyranine luminescent probes to real time measurements within the depositing film. These measurements provide a number of new insights concerning compositional evolution during film drawing including the differential evaporation of alcohol and water, the spatial mapping of the water/ethanol ratio as a function of film thickness, and the determination of the water content of the solvent at the drying line. These experiments demonstrate that luminescent organic molecules may be applied to the processing science of sol–gel thin films.

II. Experimental Methods

(1) Materials Preparation

The series of sols used in this study were synthesized with the objective of varying the amount of "excess" water in the sol. A H_2O/Si ratio of 2 is stoichiometrically sufficient to achieve complete hydrolysis and condensation of silicon alkoxides, $Si(OR)_4$, to form SiO_2 because water is produced by condensation. Even if condensation did not occur, $H_2O/Si > 4$ would result in "excess" water in the precursor sol. In this work, careful procedures were used to control the amount of excess water. The mole ratio of H_2O/Si, r, was 4 or 2.5. To make the sol, 75 mL of tetraethoxysilane (TEOS) from Fisher, 15.0 or 23.9 mL of deionized water (for $r = 2.5$ or 4.0 sols, respectively), 0.25 mL of 1*N* HCl, and 75 mL of absolute ethanol (Gold Shield) were refluxed at 65°C for 1.5 h. The volume of the mixture was then reduced by 50% by rotary evaporation to remove excess water present as the azeotrope, and an equivalent amount of absolute ethanol was added. The evaporation/reconstitution step was repeated 4 times to remove any excess water and acid. This precursor sol was then stored at 4°C until use. Immediately before the film drawing experiments, the sol was combined with an equal volume of absolute ethanol containing pyranine (Kodak Chemicals) at a concentration of $2 \times 10^{-4}M$, and then deionized water was added to bring the sol to the desired composition. The films investigated in this study were drawn from the $r = 2.5$ and 4.0 sols with 2.5, 5, 12.5 and 25 vol% of water added. From this series of sols, it was possible to examine the effect of excess water content on film composition. In addition to the silica sols, a series of ethanol/water solutions ranging from 0% to 100% in increments of 10 vol% were prepared for use as standards. The concentration of pyranine in the standard solutions ($1 \times 10^{-4}M$) was comparable to the pyranine concentration in the sol prior to film drawing.

The films were drawn using the apparatus described by Hurd and Brinker.[6] This approach uses hydraulic motion to produce a steady, vibration-free withdrawal which does not cause optical irregularities in the film. The substrates were polished strips (10 cm × 1 cm × 1 mm) of single-crystal ⟨100⟩ silicon cleaned with Chromerge (Manostat), rinsed with deionized water and then methanol and acetone. These substrates were connected to a weighted float in a water reservoir whose drainage rate was controlled by a flow valve. The apparatus for film pulling is shown in Fig. 2. The substrate was withdrawn in a chamber that was closed to the atmosphere except for a small aperture required for the excitation laser and the collecting lens. The convection-free drying of the film was critical to obtaining high

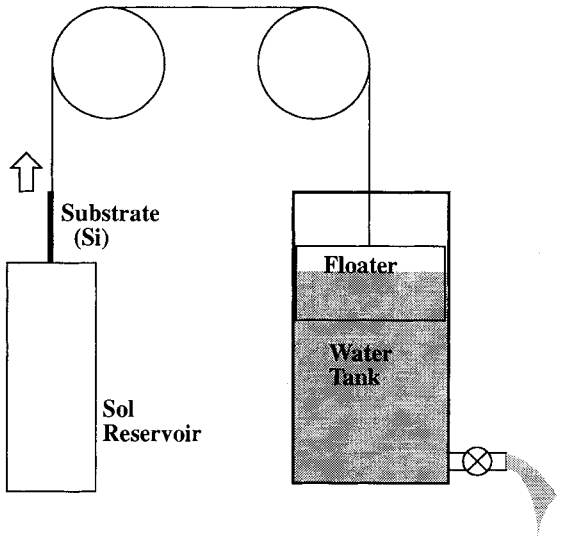

Fig. 2. Schematic of the dip-coating apparatus which uses hydraulic motion to produce vibration-free withdrawal.

optical quality films. A film drawing rate of 5 cm/min (±10%) was used for all experiments. Using this drawing rate, steady-state conditions for film deposition were established within 15 s and maintained for over a minute so that several spectra were obtained for a given substrate withdrawal. After deposition, the refractive index and thickness of the ambient-dried films were measured (*vide infra*). The substrates were not re-used.

(2) Optical Measurements

The primary experiments combined interferometry with luminescence spectroscopy to characterize spatially the chemical composition of the solvent during film pulling. The experimental arrangement is shown in Fig. 3. Interferometry was used to monitor film thickness. A mercury lamp filtered to emit 546-nm light was placed at an angle of 65° to the substrate normal to illuminate the film. A telescopic microscope at an angle of 65° to the substrate normal was used to observe fringes in the film. Interference occurs at thicknesses corresponding to

$$h = \frac{(2m + 1)\lambda}{4(n^2 - \sin^2 \theta_L)^{1/2}} \quad (1)$$

where h is the film thickness, m is the interference fringe number ($m = 0$ corresponds to the drying line), θ_L is the illumination/viewing angle of the interference pattern, and n is the refractive index of the solvent. The interference fringes were reproducible with identical pulling conditions. The fringe number not only gives film thickness according to Eq. (1), but also provides a convenient vertical scale to identify the distance between the drying line and the film reservoir or bath meniscus ($m \approx 10$ to 15 depending upon the film drawing rate).

The fluorescence was excited by the 351-nm line from a Coherent Innova 90 Ar^+ laser at a power of approximately 20 mW. The spot size of the excitation beam was less than 50 μm, allowing for excellent spatial resolution. The spectra were recorded using an EG&G Model 1420 optical multichannel analyzer (OMA) and a 0.32-m Jobin-Yvon/ISA monochromator for dispersion. The slit width was 200 μm and the integration time was 1 s. These excitation/detection conditions produced excellent quality spectra as shown in this paper. The laser spot did not affect the pattern of the interference fringes, thus indicating that local heating did not influence film quality.

The second type of experimental measurement combined interferometry with fluorescence depolarization. The fluorescence depolarization technique uses polarized light to excite a fluorescent probe molecule.[19] The probe molecules in the proper orientation will absorb the light and then luminesce at a later time, which is dependent upon their emission lifetime. The random tumbling of the probe in its excited state during this time serves to depolarize the resulting emission. The scrambling of the emission polarization is expressed as P, the degree of polarization:

$$P = \frac{I_{\parallel} - I_{\perp}}{I_{\parallel} + I_{\perp}} \quad (2)$$

where $I_{\parallel}$ and $I_{\perp}$ are the emission intensities parallel and perpendicular to the polarization of the exciting light. When the probe is free to tumble on time scales short compared to the emission process, $I_{\parallel} = I_{\perp}$ and $P = 0$. When the emitter is immobilized, P can have a value between −0.33 and +0.5. Previously, fluorescence depolarization was used to determine local viscosity and rigidity changes in sol–gel matrices.[20] In the present study,

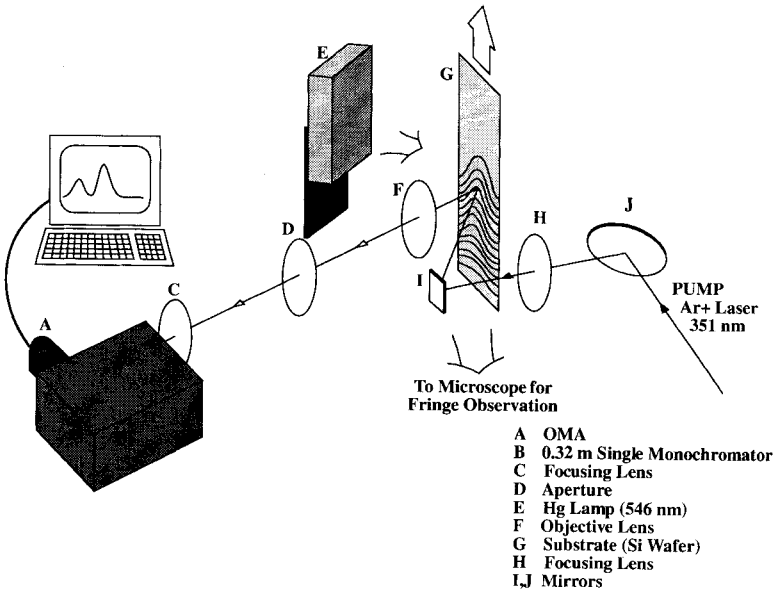

Fig. 3. Experimental arrangement combining interferometry with fluorescence spectroscopy. Components are as follows: (A) optical multichannel analyzer, (B) monochromator, (C) focusing lens, (D) aperture, (E) mercury lamp with filter (546 nm), (F) objective lens, (G) substrate (silicon wafer), (H) focusing lens, (I,J) mirrors.

this technique was used to distinguish between pyranine molecules that were free to rotate and those that were immobilized. The experiment used polarized emission (351 nm) from the argon ion laser (50:1 vertical polarization) to excite the molecule. Polarized fluorescence spectra were recorded with the computer-controlled monochromator/OMA system mentioned above. A Glan-Thompson polarizer was used as an analyzer.

(3) Characterization of Dried Films

Ellipsometry was used to measure both the thickness and the refractive index of the ambient-dried films made by sol–gel film deposition on silicon substrates.[21] Additional characterization of surface area and pore distribution was carried out by using the surface acoustic wave technique developed by Frye *et al.*[22] For these measurements, the silica films were prepared under identical deposition conditions, but with a different substrate, a single-crystal quartz substrate onto which were evaporated interdigitated gold electrodes.

III. Results

(1) Reference Spectra of Pyranine in Ethanol/Water Solutions

Luminescence spectra of pyranine in ethanol/water solutions of known composition were measured. The emission bands were broad and featureless, with two distinct peaks at 430 and 515 nm. The emission intensity at 515 nm increased relative to the intensity at 430 nm as the water increased as shown in Fig. 4. The luminescence of a pure water solution of pyranine had almost no peak at 430 nm, while in an absolute ethanol solution of pyranine the peak at 515 nm was not visible. The ratio of the heights of these two peaks served as standards by which we quantified the relative amounts of water and ethanol during the dip-coating process of sol–gel films (*vide infra*). The isobestic point attests to the fact that the peaks arise from different species (i.e., the protonated and deprotonated forms); thus the ratio of the peak heights is directly proportional to the water/ethanol ratio. It is significant to note that peak ratio methods eliminate the effects of certain measurement variables such as laser intensity, collection optics, and pyranine concentration. Although the results are not shown in this paper, it also was established that luminescence occurred when thin films of ethanol/water solutions containing pyranine were probed by the excitation beam from the Ar^+ laser.

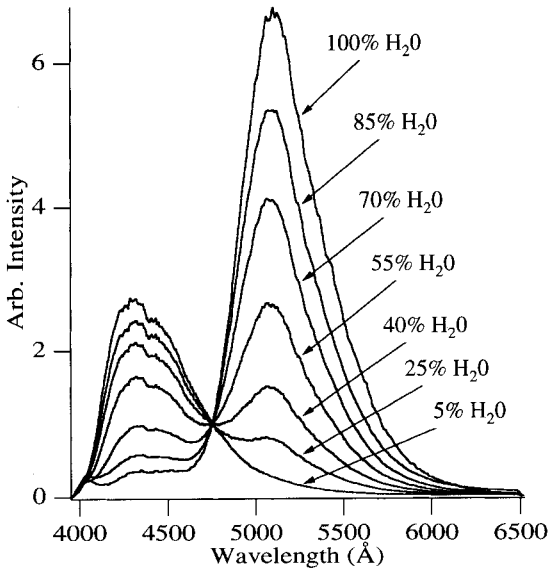

Fig. 4. Luminescence spectra of pyranine for a series of ethanol/water solutions. The volume percent of water for each spectrum is indicated. The excitation source was the 351-nm line from an Ar^+ laser.

(2) Interferometry

The characteristic interference pattern for the sol–gel film as it is withdrawn from the reservoir is shown in Fig. 5. The dynamics of the dip-coating process and the sequential stages of structural development in sol–gel films from this technique have been well reviewed.[5,23] This pattern is similar to that obtained in the imaging ellipsometry measurements reported by Hurd and Brinker.[6] The first fringe occurs in the vicinity of the drying line ($m = 0$) where the film attains its final thickness (130 to 160 nm in the present investigation). The featureless region above the first fringe, at the top of the substrate, represents a nearly dry film. The fringes offer a convenient vertical scale between the sol reservoir and the drying line, and a series of emission spectra of pyranine in silica sols of known composition were obtained at different fringe positions. The spectra were obtained as the silicon substrate was withdrawn at a constant speed from the reservoir and after the interference pattern had stabilized (i.e., steady-state conditions).

(3) Luminescence of Pyranine in Silica Sols during Film Deposition

Typical luminescence spectra at different fringe positions (or fringe numbers) are shown in Fig. 6 for a sol with a composition of $r = 4.0$. The emission spectrum of the pyranine probe changes with the position of the excitation beam. In the region closest to the reservoir, the 430-nm emission predominates, indicating low water content. The 515-nm emission becomes more prominent in the regions closer to the drying line and, just below the drying line, this emission dominates, signaling an increased water content. Then, just above the drying line, the 430-nm emission is again the strongest, suggesting a decreased water content. As will be shown in the discussion section, this enhanced blue peak arises from lack of solvation and not from low water content in the solvation shell of the molecule.

The spectral data shown in Fig. 6 can be converted to a more quantitative form by comparing the ratio of the 430- and 515-nm peaks to the ratio of the pyranine peaks shown in the reference spectra (Fig. 4). Figure 7 illustrates how the water content in the film varies between the reservoir and the drying line. There are two important features shown here. First, it is evident that the film exhibits a rapid increase in water content

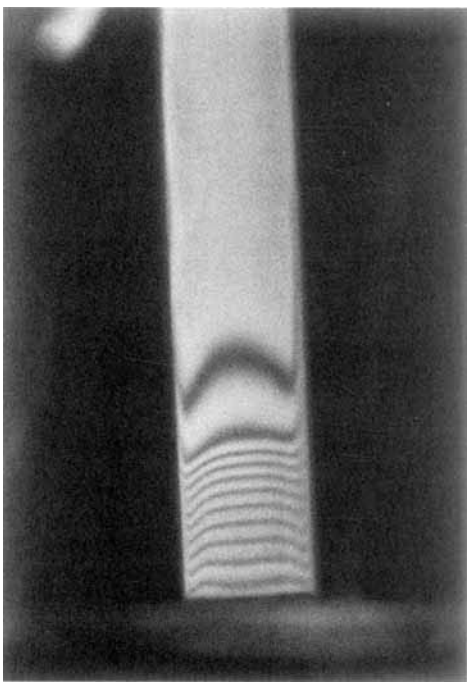

Fig. 5. Photograph showing the characteristic interference pattern which occurs as the sol–gel film is withdrawn from the reservoir. The drying line is in the vicinity of the uppermost fringe.

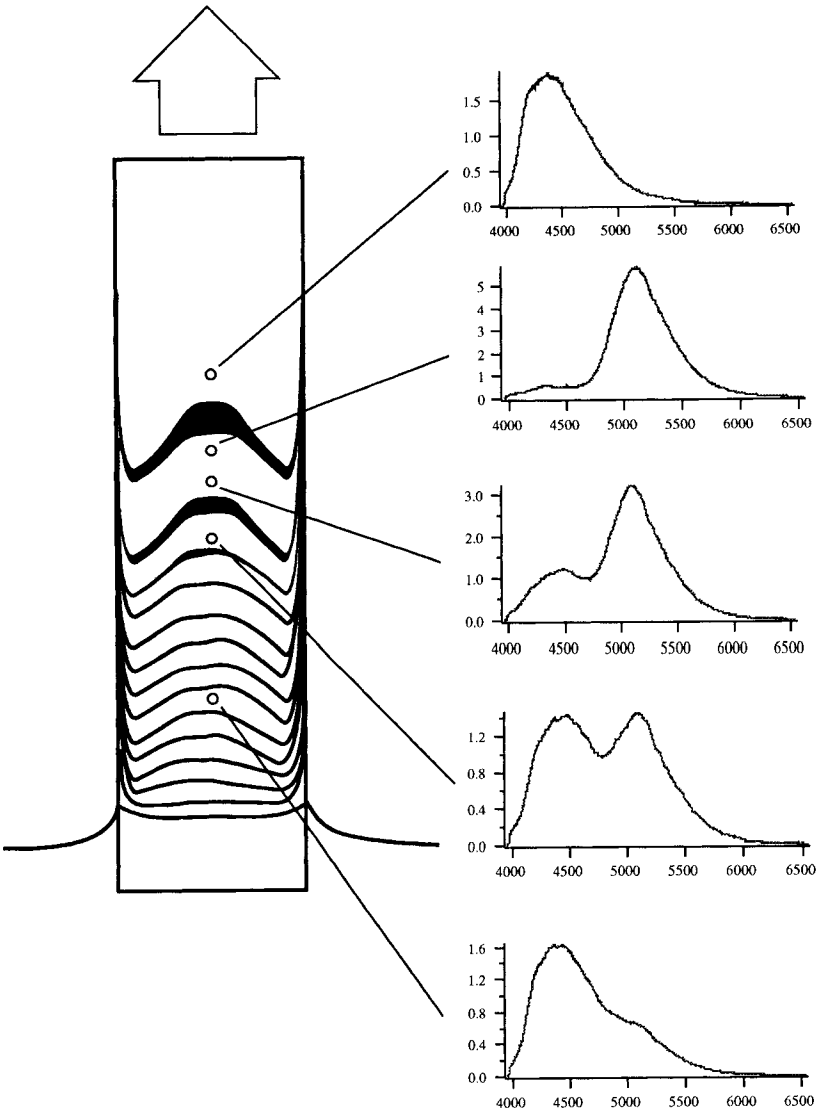

Fig. 6. Luminescence spectra at various fringe positions for a film deposited from a sol with $r = 4.0$ and 12.5% excess water added.

as the drying line is approached. This sharp gradient is comparable for all the sol/water systems measured: from 2.5% excess water to 25% excess. It is significant to note that, although preferential evaporation of EtOH has been proposed,[24] this work represents the first time it has been observed experimentally.

The second point to be considered is that the maximum water content in the immediate vicinity of the drying line depends upon the excess water content in the sol. This value ranges from 50% with 2.5% excess water to 85% at 25% excess. Interestingly, there is nearly no change in maximum water content or the composition gradient for the sols prepared with 12.5% and 25% excess water. The water content in the vicinity of the drying line has significant implications for sol–gel films prepared by dip coating. The greater surface tension of water causes a corresponding increase in capillary pressure which is instrumental in the dynamics of film formation and the structural development of sol–gel films.[5]

(4) Properties of Dried Films

In this series of measurements we determined the refractive index and film thickness in an attempt to investigate how the chemistry of the sol influences the structural development of the dip-coated films. The results are shown in Fig. 8. The refractive index (632.8 nm) is approximately 1.43 and is virtually independent of the excess water content of the sol. Over this same range the film thickness exhibits some variation, 1650 to 1350 Å, or ≈20%. The thickness increases with additions in water content but then decreases at the highest level prepared, 25%. Since the refractive index is a measure of porosity, these results suggest that film porosity is practically unaffected by the water content of the sol and, correspondingly, the variation in film thickness cannot be attributed to changes in porosity. This somewhat surprising result may reflect the competition of factors that promote collapse of the network during drying and those that resist this collapse. Enriching the pore fluid in water causes the surface tension to increase, which should increase the capillary pressure and the extent of collapse of the gel. However, water also tends to promote further condensation reactions and coarsening which tend to strengthen the gel. These competing features are likely to be the principal factors responsible for the observed refractive index behavior.

IV. Discussion

We have used the emission characteristics of pyranine to determine the solvent composition in sol–gel thin films as they are withdrawn from the sol reservoir. The emission spectra of pyranine depend on whether or not the molecule is protonated. Adding water to an alcohol solution will increase the number of deprotonated pyranine species and, therefore, the intensity of the luminescence peak at 515 nm. From this protonation/deprotonation behavior, we have been able to quantify chemical changes in the solvent during film pulling, to map spatially the

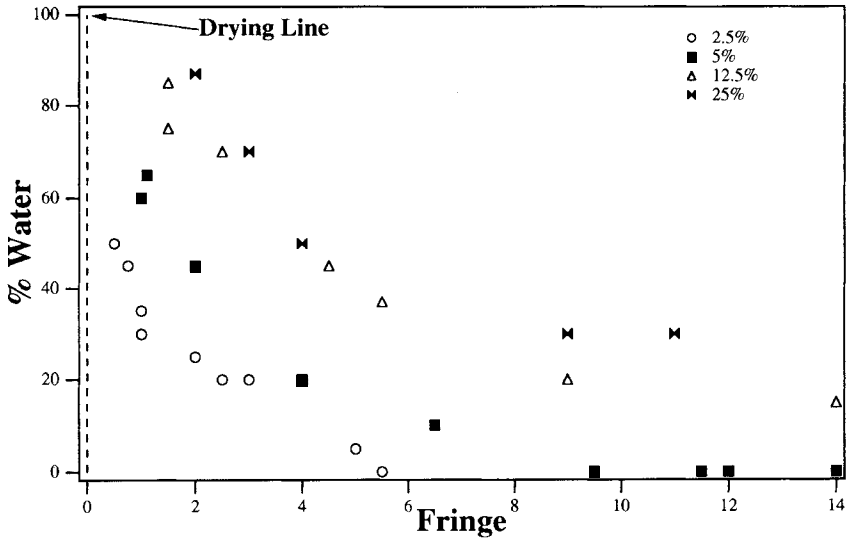

Fig. 7. Water content (vol%) in the film as a function of fringe number for several $r = 4.0$ sols containing different amounts of excess water: 2.5, 5, 12.5, and 25 vol%. The drying line is at $m = 0$. The films were drawn at a rate of 5 cm/min.

volumetric water/ethanol ratio in films in real time, and to investigate how the solvent composition in the film is influenced by the overall composition of the sol.

(1) Composition of Silica Sols from Pyranine Luminescence

The results reported here are the first ones to show definitively that there is preferential loss of ethanol during film deposition (Fig. 6). This effect has been widely assumed and even used in developing models for the dip-coating process.[24] The present experiments prove the effect and quantify the gradient produced.

The increase in the water content of the solvent is due to physical processes (i.e., preferential evaporation of ethanol) rather than chemical processes associated with the production or consumption of water during condensation or hydrolysis. Calculations have shown how preferential evaporation of EtOH leaves behind a water-rich film in the vicinity of the drying line.[24] The results for TEOS/EtOH/H_2O sols (Fig. 7) are consistent with this model. From the chemical perspective, hydrolysis

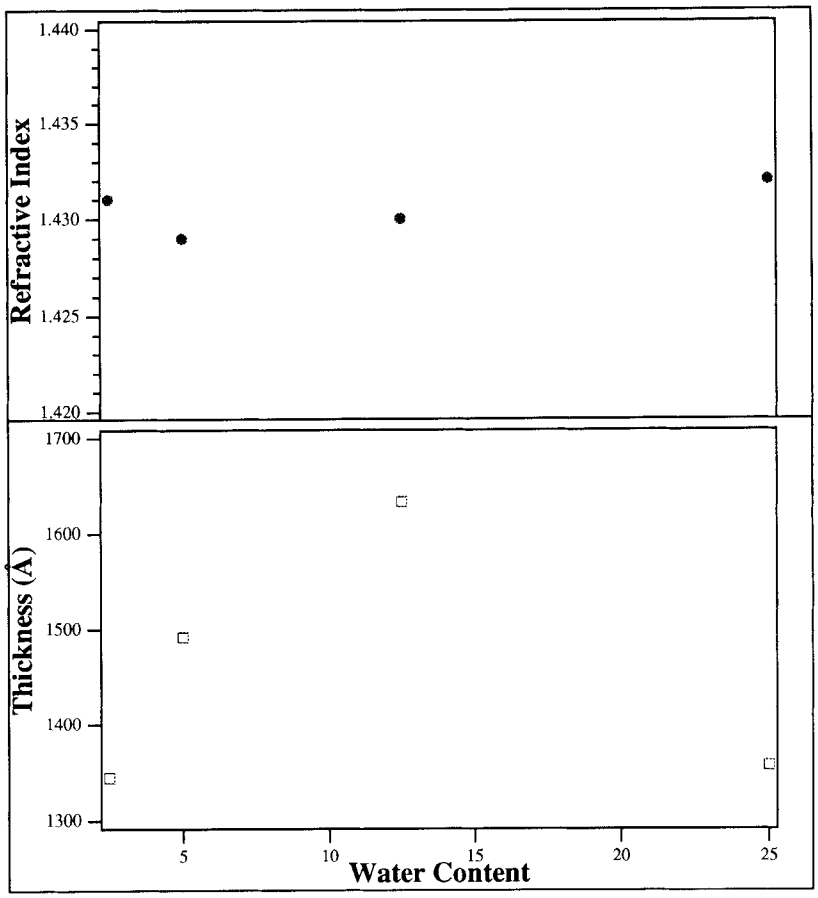

Fig. 8. Refractive index and thickness of dried films as a function of the excess water content (vol%) for $r = 4.0$ sols.

was complete after the sols were synthesized and any water produced from condensation during synthesis was removed by rotary evaporation. Even if the 4:1 (H_2O:Si) sol had no condensation until film deposition, the water produced by condensation would not exceed more than a few volume percent in the sol. This amount is insignificant compared to the large increase in water content observed within the first few fringes of the drying line.

The measurements of film water content are quite significant in that the compositional information is obtained spatially and in real time (i.e., as the film is being drawn). The compositional profile can be derived as a function of film thickness. Through the use of Eq. (1), the fringe number can be used accurately to calculate film thickness. A compositional profile of the film prepared using the sol with 5% excess H_2O is shown in Fig. 9. This curve is analogous to that of Fig. 7 except that now the solvent composition at a given thickness is known. Moreover, since the overall composition of the sol affects the water concentration gradient (Fig. 7), it is evident that the water content thickness profile will be influenced by the specific sol composition.

The results in Fig. 9 underscore an important part of this research: the applicability of this work to thin-film process control. The use of an optical signal to monitor the chemical composition and film thickness provides an opportunity to control rigorously film processing through automated methods. Although the results are obtained for dip coating, it is evident that these methods may be readily adapted to other solution-based materials preparation processes such as fiber spinning.

(2) Water Content at the Drying Line

Two effects become evident in the vicinity of the drying line (Fig. 6). The emission at 515 nm first becomes dominant (suggesting high water content) and then decreases as the compositional profile is traced from the sol reservoir (or gravitational meniscus) to the drying line. The maximum water content occurs either at or just below the first interference fringe. As shown in Fig. 7, the magnitude of the maximum is influenced by the excess water content of the sol. Since the surface tension is affected by the water/ethanol ratio, the water content at the drying line is likely to affect the capillary pressure exerted during the drying stage.[5] The influence of sol composition on dried films is discussed more fully in the following section.

The spectral results suggest an apparent decrease in water concentration at and above the drying line. This effect, however, arises from loss of the liquid phase rather than from a change in solvent composition. The loss of the liquid can be shown by polarized emission measurements. Such experiments reflect the ability of the probe molecule to reorient while it is in its excited state. When excited by polarized light, the emission of a fully solvated or rotating molecule is depolarized; there is no difference in emission intensity regardless of analyzer position ($I_{\parallel} = I_{\perp}$). This behavior is observed at all the interference fringes below the drying line. Figure 10 gives the polarized emission spectra a short distance above the gravitational meniscus. The spectra are those of a solvated protonated species (peak at 430 nm) whose motions are unrestricted ($P = 0$). Polarized spectra taken closer to the drying line, but below the first interference fringe, also exhibit $P = 0$. These emission spectra have a pronounced peak at 515 nm because of the increase in water content of the solvent phase as the drying line is approached.

An immobilized molecule is not free to rotate and will exhibit polarized emission. The polarized emission spectra in the vicinity of the drying line (Fig. 11) indicate that there are two different types of environments for the pyranine molecules. There are water-solvated molecules characterized by the 515-nm emission peak and $P = 0$. In the absence of solvent, the proton does not dissociate, and the pyranine molecules remain protonated and have luminescence spectra similar to that of ethanol. These pyranine molecules not only exhibit the 430-nm emission, but also possess a high value of polarization ($P = -0.33$), indicating that these molecules are largely immobilized. Thus, the polarized emission measurements show that, in the region of the drying line, the final solvent evaporates and the pyranine probe molecules are left adsorbed on the silica surface. The observed increase in the blue emission during film drying is consistent with prior work on pyranine-doped monoliths where solvent removal by vacuum heat treatment resulted in a predominantly blue emission.[14]

(3) Relationship of Sol Chemistry to the Properties of Dried Films

It is interesting to examine the properties of dried films and to determine the extent to which the physical properties of the films are influenced by the chemistry of the sol. In general, these types of studies have received little attention. Prior work on sol–gel films showed that the amount of excess water added to the sol influenced the refractive index. These results were interpreted in terms of two competing effects, as both capillary pressure and stiffening of the silica network are enhanced with increasing water content.[23]

In the dip-coating process, there is very little time available for condensation reactions to occur. The weakly branched precursors can interpenetrate and are easily compacted by evaporation into a densely packed, compliant network with molecular-size pores. The capillary pressure (C_p) exerted during the drying stage is extremely large because of the small pores:

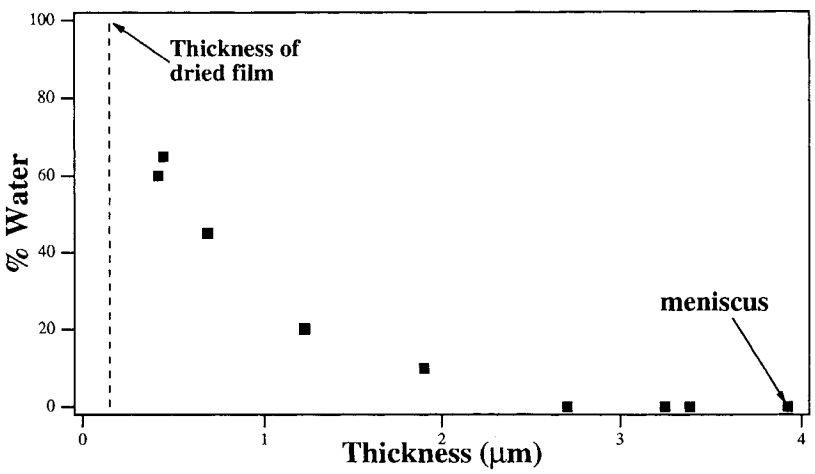

Fig. 9. Spatial map showing the water content (vol%) of the solvent in the film as a function of film thickness for the $r = 4.0$ sol with 5% excess water drawn at a rate of 5 cm/min.

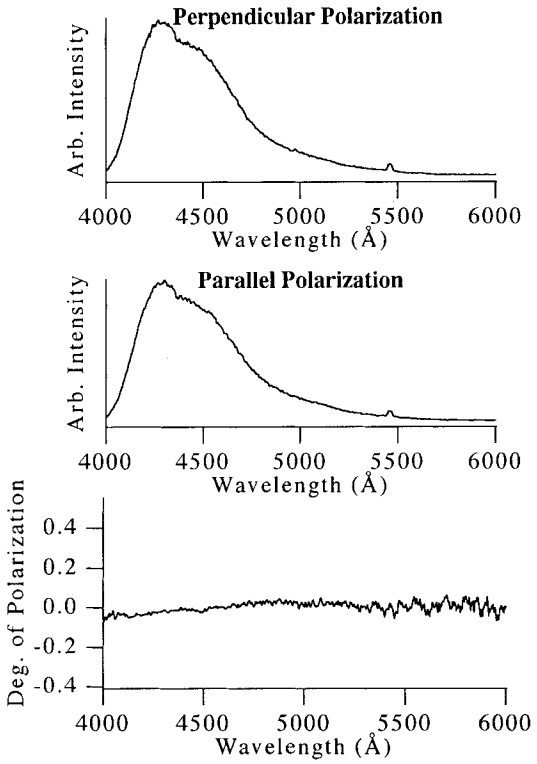

Fig. 10. Polarized emission spectra for a sol–gel film taken near the sol reservoir. The emission is shown polarized perpendicular (top) and parallel (middle) to the incident laser beam. The degree of polarization is obtained accordingly (bottom). The sol composition was $r = 2.5$ with 5% excess water and the film was drawn at 5 cm/min. The small peak at ≈545 nm is a plasma line from the Ar^+ laser.

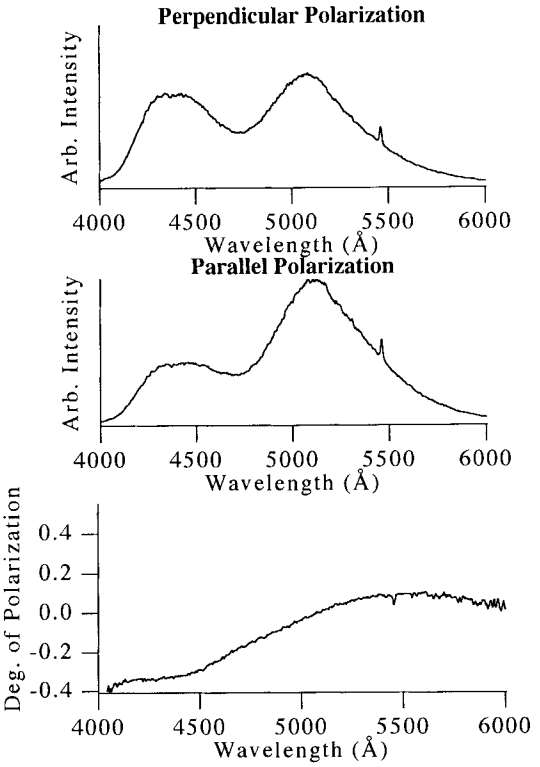

Fig. 11. Polarized emission spectra for the same sol–gel film shown in Fig. 10 taken in the vicinity of the drying line. The small peak at ≈545 nm is a plasma line from the Ar^+ laser.

$$C_p \propto \frac{-\gamma_{LV}}{r_p} \tag{3}$$

where γ_{LV} is the liquid–vapor surface tension and r_p is the pore radius.

The sols prepared for the present investigation were designed to be as fully hydrolyzed as possible by the use of refluxing and rotary evaporation. In this way there would be no excess water present in the sol prior to the addition of the various water/alcohol mixtures immediately before film deposition. It was expected that this synthesis approach would provide a means of studying the effects of capillary forces on the densification of films. However, it should be restated that the effect of water on film properties is twofold: (1) it increases the value of the surface tension (γ_{LV}) and, therefore, the capillary pressure; (2) it has a tendency to strengthen the gel and thus increase the gel's resistance to collapse.

The experimental results on the dried films (Fig. 8) are characterized by two distinct features; the refractive index values are virtually independent of sol composition (even at 0% water) and the magnitude of the refractive index is representative of a rather dense film. These results suggest that the two water-induced effects compensate for each other. The relative network stiffening is measured by the elastic modulus which is proportional to $(\phi_0/\phi)^{3.8}$, where ϕ is the volume fraction solids during drying and ϕ_0 is the volume fraction at the gel point. One possible explanation for the results shown in Fig. 8 is that the sol compositions are in a limiting condition where the modulus has become so large that further pore shrinkage is arrested. The high value of the refractive index is consistent with this explanation as the refractive index scales with the volume fraction of solids.[5] The high refractive index value obtained at 0% water added (i.e., no water is added to the sol after hydrolysis) arises from a different consideration. In this case, the high refractive index may be a consequence of ethoxylation of pore surfaces that occurs under these synthesis conditions. Fully ethoxylated surfaces cannot react during drying and will foster collapse of the network as solvent is removed.

The effect of sol composition on film thickness will be strongly influenced by the rheology of the sol. For films of approximately the same refractive index, the thickness, h, should be proportional to the thickness of the film entrained during dip coating:

$$h \propto \frac{0.94\,(\eta U)^{2/3}}{\gamma_{LV}^{1/6}(\rho g)^{1/2}} \tag{4}$$

where U is the coating speed, η is the viscosity, g is the gravitational constant, and ρ is the density of the sol. The liquid–vapor surface tension (γ_{LV}) changes with water content, but this is not likely to have a significant effect because of the weak power-law dependence. Instead, the change in sol viscosity is the most important factor. The rheological properties of suspensions are often concentration dependent and exhibit different flow regimes (e.g., Newtonian, thixotropic).[26] In particular, the sol with 25% water added exhibited a noticeably lower viscosity than the other systems, and the corresponding thinner coating obtained with this composition is consistent with this observation. The observed increase in film thickness with increase in water content (0% to 12.5%) could also be a viscosity–related effect and the precise mechanism by which thicker films are produced is presently under investigation.

V. Conclusions

This paper has demonstrated that pyranine may be used as a fluorescence probe to monitor the chemical evolution *in situ* during sol–gel thin film deposition of silica by the dip-coating process. An important consideration in this work is that fluorescence spectroscopy represents an effective analytical method over dimensions in the 1000-Å range. The sensitivity of the pyranine luminescence to protonation/deprotonation effects was used to quantify changes in the alcohol/water ratio within the depositing film as the substrate was withdrawn from the sol reservoir.

These measurements provide a number of new insights concerning the chemical changes which occur during film deposition. The spatially resolved spectral results clearly show for the first time that differential evaporation of alcohol and water causes the composition of the entrained sol to become progressively enriched in water with increasing distance from the reservoir surface. The water content of the solvent near the drying line is dependent upon the water content of the initial sol, and values in excess of 80 vol% water were observed in the vicinity of the drying line. By correlating the luminescence results with the interference pattern of the depositing film, it is possible to map the solvent composition as a function of film thickness. These results are of considerable significance from the standpoint of automated process control. The use of an optical signal to monitor chemical composition and film thickness in real time offers an opportunity to control rigorously film processing through computer-based methods.

Acknowledgment: We thank Carol S. Ashley for technical assistance in preparation of some of the coating sols.

References

[1]L. L. Hench and J. K. West, "The Sol–Gel Process," *Chem. Rev.*, **90**, 33–72 (1990).

[2]C. J. Brinker and G. Scherer, *Sol–Gel Science: The Physics and Chemistry of Sol–Gel Processing*. Academic Press, San Diego, CA, 1990.

[3]L. C. Klein (Ed.), *Sol–Gel Technology*. Noyes Publications, Park Ridge, NJ, 1988.

[4]D. R. Uhlmann and G. P. Rajendran, "Coatings: The Land of Opportunity for Sol–Gel Technology"; p. 241 in *Ultrastructure Processing of Advanced Ceramics*. Edited by J. D. Mackenzie and D. R. Ulrich. Wiley, New York, 1988.

[5]C. J. Brinker, A. J. Hurd, G. C. Frye, P. R. Schunk, and C. S. Ashley, "Sol–Gel Thin Film Formation," *J. Ceram. Soc. Jpn.*, **99**, 862–77 (1991).

[6]A. J. Hurd and C. J. Brinker, "Ellipsometric Imaging of Drying Sol-Gel Films," *Mater. Res. Soc. Symp. Proc.*, **121**, 731–42 (1988).

[7]D. Avnir, S. Braun, and M. Ottolenghi, "The Encapsulation of Organic Molecules and Enzymes in Sol–Gel Glasses: Novel Photoactive, Optical, Sensing and Bioactive Materials,"; pp. 384–404 in ACS Symposium Series, Vol. 499, *Supramolecular Architecture*. Edited by T. Bein. American Chemical Society, Washington, DC, 1992.

[8]B. Dunn and J. I. Zink, "Optical Properties of Sol–Gel Glass Doped with Organic Molecules," *J. Mater. Chem.*, **1**, 903–13 (1991).

[9]R. Reisfeld and C. K. Jorgensen; pp. 207–56 in *Structure and Bonding*, Vol. 77. Edited by R. Reisfeld and C. K. Jorgensen. Springer-Verlag, Geneva, Switzerland, 1992.

[10]V. R. Kaufman and D. Avnir, "Structural Changes along the Sol–Gel–Xerogel Transition in Silica as Probed by Pyrene Excited-State Emission," *Langmuir*, **2**, 717–22 (1986).

[11]D. Avnir, D. Levy, and R. Reisfeld, "The Nature of the Silica Cage as Reflected by Spectral Changes and Enhanced Photostability of Trapped Rhodamine 6G," *J. Phys. Chem.*, **88**, 5956–59 (1984).

[12]J. M. McKiernan, S. A. Yamanaka, E. T. Knobbe, J. C. Pouxviel, S. Parveneh, B. Dunn, and J. I. Zink, "Luminescence and Laser Action of Coumarin Dyes Doped in Silicate and Aluminosilicate Glasses Prepared by the Sol–Gel Technique," *J. Inorg. Organomet. Polym.*, **1**, 87–103 (1991).

[13]V. R. Kaufman, D. Avnir, D. Pines-Rojanski, and D. Huppert, "Water Consumption During the Early Stages of the Sol–Gel Tetramethyl Orthosilicate Polymerization as Probed by Excited State Proton Transfer," *J. Non-Cryst. Solids*, **99**, 379 (1988).

[14]J. C. Pouxviel, B. Dunn, and J. I. Zink, "Fluorescence Study of Aluminosilicate Sols and Gels Doped with Hydroxy Trisulfonated Pyrene," *J. Phys. Chem.*, **93**, 2134–39 (1989).

[15]J. M. McKiernan, J. C. Pouxviel, B. Dunn, and J. I. Zink, "Rigidochromism as a Probe of Gelation and Densification of Silicon and Mixed Aluminum–Silicon Alkoxides," *J. Phys. Chem.*, **93**, 2129–33 (1989).

[16]N. R. Clement and M. Gould, "Pyranine as a Probe of Internal Aqueous Hydrogen Ion Concentration in Phospholipid Vesicles," *Biochemistry*, **20**, 1534–38 (1981).

[17]K. Kano and J. H. Fendler, "Pyranine as a Sensitive pH Probe for Liposome Interiors and Surfaces; pH Gradients Across Phospholipid Vesicles," *Biochim. Biophys. Acta*, **509**, 289–99 (1978).

[18]O. S. Wolfbeis, E. Fürlinger, H. Kroneis, and H. Marsoner, "A Study on Fluorescent Indicators for Measuring Near Neutral pH Values," *Fresnius' Z. Anal. Chem.*, **314**, 119–24 (1983).

[19]B. Weib Van der Meer; pp. 1–31 in *Subcellular Biochemistry*. Edited by H. Hiderson. Plenum, New York, 1986.

[20]J. M. McKiernan, J. I. Zink, and B. Dunn, "Fluoresence Depolarization Studies of Sol–Gel Derived Glasses Using a Rigidochromic Probe"; pp. 381–86 in Proceedings of SPIE, Vol. 1758, *Sol–Gel Optics II*. Edited by J. D. Mackenzie. International Society for Optical Engineering, Bellingham, WA, 1992.

[21]R. A. Weimer, P. M. Lenahan, T. A. Marchione, and C. J. Brinker, "Electronic Properties of Sol–Gel Derived Oxides on Silicon," *Appl. Phys. Lett.*, **51**, 1179 (1987).

[22]G. C. Frye, A. J. Ricco, S. J. Martin, and C. J. Brinker, "Characterization of the Surface Area and Porosity of Sol–Gel Films Using SAW Devices," *Mater. Res. Soc. Symp. Proc.*, **121**, 349 (1988).

[23]A. J. Hurd and C. J. Brinker, "Sol–Gel Film Formation by Dip Coating," *Mater. Res. Soc. Symp. Proc.*, **180**, 575–81 (1990).

[24]P. R. Schunk, A. J. Hurd, and C. J. Brinker, "Free Meniscus Coating Process"; in *Liquid Film Coating, Scientific Principles and Their Technological Implications*. Edited by P. M. Schweizer and S. F. Kistler. Chapman and Hall, New York, in press.

[25]C. J. Brinker, A. J. Hurd, G. C. Frye, P. R. Schunk, and C. S. Ashley, "Sol–Gel Thin Film Formation"; pp. 395–413 in *Chemical Processing of Advanced Materials*. Edited by L. L. Hench and J. K. West. Wiley, New York, 1992.

[26]S. Sakka and K. Kamiya, "Formation of Sheets and Coating Films from Alkoxide Solutions," *J. Non-Cryst. Solids*, **48**, 31 (1982). □